Published in final edited form as:

Cell Rep. 2017 September 26; 20(13): 3212–3222. doi:10.1016/j.celrep.2017.08.099.

The E3 ubiquitin ligase SCF(Cyclin F) transmits AKT signaling to the cell cycle machinery

Rajarshi Choudhury[1,2], **Thomas Bonacci**[1], **Xianxi Wang**[1], **Andrew Truong**[1,2], **Anthony Arceci**[1,4], **Yanqiong Zhang**[1], **Christine A Mills**[1,2], **Jennifer L Kernan**[1,2], **Pengda Liu**[1,3], and **Michael J Emanuele**[1,2,3,*]

[1]Lineberger Comprehensive Cancer Center, The University of North Carolina at Chapel Hill, Chapel Hill, NC 27599

[2]Department of Pharmacology, The University of North Carolina at Chapel Hill, Chapel Hill, NC 27599

[3]Department of Biochemistry and Biophysics, The University of North Carolina at Chapel Hill, Chapel Hill, NC 27599

[4]Curriculum in Genetics and Molecular Biology, The University of North Carolina at Chapel Hill, Chapel Hill, NC 27599

SUMMARY

The oncogenic AKT kinase is a key regulator of apoptosis, cell growth and cell cycle progression. Despite its important role in proliferation, it remains largely unknown how AKT is mechanistically linked to cell cycle. We show here that Cyclin F, a substrate receptor F-box protein for the SCF family of E3 ubiquitin ligases, is a *bona fide* AKT substrate. Cyclin F expression oscillates throughout the cell cycle, a rare feature among the 69 human F-box proteins, and all of its known substrates are involved in proliferation. AKT phosphorylation of Cyclin F enhances its stability and promotes assembly into productive E3 ligase complexes. Importantly, expression of mutant versions of Cyclin F that cannot be phosphorylated by AKT impair cell cycle entry. Our data suggest that Cyclin F transmits mitogen signaling through AKT to the core cell cycle machinery. This discovery has potential implications for proliferative control in malignancies where AKT is activated.

eTOC Blurb

Choudhury *et al*. report that Cyclin F, an E3 ubiquitin ligase substrate receptor F-box protein, is phosphorylated by the oncogenic kinase AKT. Intriguingly, phosphorylation enhances Cyclin F

*Corresponding author and lead contact: emanuele@email.unc.edu.

AUTHOR CONTRIBUTIONS

MJE and RC conceptualized the project and designed experiments. RC carried out the majority of experiments. MJE, RC, and AT assembled the figures. MJE and RC wrote the paper. YZ and PL specifically helped with AKT activity experiments. TB, AA, XW, CAM and JLK carried out experiments.

stability and promotes cell cycle entry. These data suggest that Cyclin F bridges growth factor to the core cell cycle machinery.

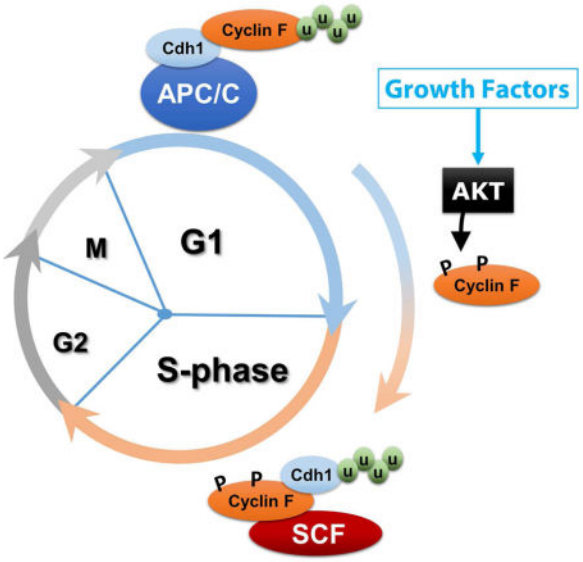

INTRODUCTION

Eukaryotic cells progress into the cell cycle in response to growth factor stimulation (Pardee, 1974; Temin, 1971). This implies that intracellular signaling pathways communicate growth factor signaling to the core cell cycle machinery. While the general molecular framework of both growth factor signaling pathways and the core cell cycle oscillator have been well-described, there remain few mechanistic links detailing how they are connected to one another. The mitogen sensing phosphatidylinositol 3-kinase (PI3K) – AKT pathway plays an important role in apoptotic evasion and cell growth. Moreover, PI3K-AKT pathway activation is a common feature in many malignancies (Manning and Toker, 2017). Despite the fact that AKT is commonly activated in cancer, and can promote cell cycle progression and transformation, very few established AKT substrates are directly linked to the cell cycle (Kandel et al., 2002; Manning et al., 2005; Skeen et al., 2006).

Cell cycle progression is driven by changes in the expression and subsequent degradation of many proteins (e.g. Cyclins). The ubiquitin proteasome system (UPS) represents the major mechanism of programmed protein degradation in eukaryotes and plays a vital role in cell cycle. Substrate specificity in the UPS is controlled by E3 ubiquitin ligases (Hershko and Ciechanover, 1998; Varshavsky, 2012). The Cullin-RING ligases (CRLs) represent the largest E3 ligase family in humans and encode several hundred unique enzymes. CRLs regulate the degradation of hundreds of proteins and have been implicated in all facets of eukaryotic biology, and particularly in proliferative control (Emanuele et al., 2011; Petroski and Deshaies, 2005). The CRLs rely on a CULLIN backbone that interacts simultaneously with substrates and E2 ubiquitin-conjugating enzymes. The CULLIN1 based CRL ligases, termed CRL1 or SCF (Skp1/Cul1/F-box), rely on a family of 69 substrate adaptors known as F-box proteins which designate targets for ubiquitylation. F-box proteins are defined by the

presence of an F-box domain which directly binds to the CULLIN1/Cul1 adaptor protein Skp1 (Bai et al., 1996; Jin et al., 2004). SCF complexes are modular in that different F-box proteins can interchangeably interact with Skp1. Substrate ubiquitylation by SCF complexes is often controlled by either post-translational modification of the substrate, which regulates binding to its cognate E3 ligase, or through changes in the abundance of the E3 ligase substrate receptor (Skaar et al., 2014; Vashisht et al., 2009; Zheng et al., 2016). However, an alternative mechanism for controlling substrate ubiquitylation is to regulate assembly of the ligase itself, as is the case for other cell cycle ubiquitin ligases (Sørensen et al., 2001; Zachariae, 1998). However, it is unknown if the assembly of specific CRL ligases is regulated to control substrate ubiquitylation.

Cyclin F is the founding member of the F-box family of SCF substrate receptors. Despite its name, Cyclin F is a non-canonical cyclin that is unable to bind or activate a CDK (D'Angiolella et al., 2013). Cyclin F is important for cell cycle progression and mouse development, but has few known substrates (Tetzlaff et al., 2004). However, all of the established Cyclin F targets are linked to cell cycle control: the RRM2 subunit of ribonucleotide reductase, spindle regulators Nusap1 and CP110, replication licensing factor Cdc6, and the DNA exonuclease Exo1 (D'Angiolella et al., 2010, 2012; Elia et al., 2015; Emanuele et al., 2011; Tetzlaff et al., 2004; Walter et al., 2016).

We recently demonstrated that Cyclin F is targeted for degradation during G1 phase by a cell cycle E3 ubiquitin ligase termed the Anaphase Promoting Complex/Cyclosome (APC/C) (Choudhury et al., 2016). Cdh1/Fzr1, the substrate receptor for the APC/C during G1 phase, is critical for mediating Cyclin F degradation. Surprisingly, we found that Cdh1 is itself a substrate for SCF(Cyclin F) in late G1 and during S-phase. This direct, reciprocal relationship between the APC/C and SCF(Cyclin F) represents an important negative feedback circuit regulating cell cycle progression. Interestingly, Cyclin F accumulation begins in late G1 when APC/C(Cdh1) is presumably still active (Choudhury et al., 2016).

How Cyclin F evades APC/C mediated degradation was unclear. We therefore sought to determine factors that enhance SCF(Cyclin F) dependent degradation of Cdh1 at the expense of the reverse reaction (i.e. APC/C dependent degradation of Cyclin F; Figure 1A). We considered phosphorylation of either Cyclin F or Cdh1 due to its well-established role in mediating protein ubiquitylation and degradation. Human Cyclin F contains two optimal AKT consensus motifs that are conserved evolutionarily. Moreover, AKT activity oscillates throughout the cell cycle and promotes cell cycle progression (Liu et al., 2014; Shtivelman et al., 2002; Skeen et al., 2006). Here we describe the control of Cyclin F by the oncogenic, cell cycle regulated kinase AKT.

RESULTS

Cyclin F is an AKT substrate

A recent report demonstrated that AKT kinase activity increases throughout the cell cycle (Liu et al., 2014). Consistent with this report, we found that phosphorylation of both threonine 308 and serine 473 in AKT, which contribute to AKT activity, oscillate during cell cycle progression while total AKT levels remain unchanged (Figure 1B and Supplemental

Figure 1A). Cyclin F contains two optimal, evolutionarily conserved AKT consensus motifs (RxRxxS/T) at threonine 31 and serine 577 (Figure 1C). We therefore investigated whether Cyclin F is an AKT substrate. We evaluated their kinase-substrate relationship based the following criteria: enzyme-substrate binding, *in vitro* and *in vivo* phosphorylation, and demonstration that the sites of modification are relevant in a biological context (Dephoure et al., 2013).

We expressed Myc-tagged Cyclin F (Myc-Cyclin F) and an active version of AKT1 (HA-Myr-AKT1) in HEK-293T cells and purified AKT on anti-HA agarose (Figure 1D; cells were treated with proteasome inhibitor prior harvesting). We observed a strong co-immunoprecipitation (co-IP) between Cyclin F and AKT1 under these conditions. Likewise, when we precipitated Myc-Cyclin F, we recovered AKT1 (Figure 3D). An endogenous Cyclin F pulldown performed in 293T cell extracts co-precipitated AKT, further confirming their interaction (Figure 1E). Next, we examined the ability of AKT1 to phosphorylate Cyclin F in an *in vitro* kinase assay. Purified Cyclin F was mixed with active, recombinant GST-AKT1 isolated from bacteria. Following their co-incubation, Cyclin F phosphorylation was analyzed by immunoblotting with an antibody which recognizes phosphorylated AKT consensus motifs (RxRxxpS/T; Figure 1F). Cyclin F was readily phosphorylated under these conditions. Likewise, HA-Myr-AKT1 phosphorylated Cyclin F *in vitro* as detected using radioactive [γ-^{32}P] ATP (Supplementary Figure 1B). Furthermore, Cyclin F phosphorylation was dependent on T31 and S557, the predicted sites embedded in the two AKT consensus motifs in Cyclin F. A mutant version of Cyclin F harboring alanine substitutions at these sites (T31A, S577A; Cyclin F^{AA}) showed no appreciable phosphorylation by AKT1 in *in vitro* kinase assays (Supplementary Figure 1B).

To establish that AKT1 phosphorylates Cyclin F *in vivo*, we isolated endogenous Cyclin F from whole cell extracts and analyzed it using an AKT phospho-motif antibody and mass spectrometry. First, we immuno-precipitated and stringently washed endogenous Cyclin F from cell extracts. Immunoblotting revealed a band corresponding to the molecular weight of endogenous, phosphorylated Cyclin F that reacted strongly with an AKT phospho-motif antibody, and this was abolished by acutely pre-treating cells with the selective, small-molecule AKT inhibitor afuresertib/GSK2110183 (Figure 1G). Furthermore, the phospho-motif reactive band was not present in control IgG pulldowns and was sensitive to treatment with lambda phosphatase (Supplemental Figure 1C and 1D).

Next, we ectopically expressed Myc-Cyclin F with or without a constitutively active form of AKT (HA-Myr-AKT1) in 293T cells. Cyclin F was recovered by anti-Myc IP and analyzed by mass spectrometry (Supplementary Figure 2A and B). Phosphorylation of S577 was identified in samples where AKT1 was expressed, and the modification was enriched relative to controls. We were unable to detect phospho-peptides corresponding to the T31 site, likely because AKT phosphorylation sites are difficult to detect using conventional, trypsin-based digestion methods due to arginine residues in the vicinity of the modified serine or threonine. Taken together, these data demonstrate that Cyclin F is a *bona fide* AKT substrate.

AKT controls Cyclin F stability

To evaluate the importance of Cyclin F phosphorylation by AKT, we examined Cyclin F levels by immunoblot after depleting AKT using siRNAs. We depleted both AKT1 and AKT2 with siRNAs and compared them to cells treated with negative control oligonucleotides targeting firefly luciferase (siFF). Depletion of both AKT1 and AKT2 with multiple, unrelated siRNA oligonucleotides reduced the level of Cyclin F (Figure 2A). Consistently, expression of constitutively active HA-Myr-AKT1 significantly increased the abundance of Myc-Cyclin F (Figure 2B), together suggesting that Cyclin F levels are positively regulated by AKT. These results are consistent with observations showing that the stability of Cyclin F is altered by the pharmacological manipulation or altered expression of AKT (described below).

We examined whether AKT regulates Cyclin F stability. AKT1 and AKT2 were depleted from 293T cells by siRNAs and cells were treated with the protein translation inhibitor cycloheximide (CHX). Semi-quantitative analysis of immunoblots performed on these experiment indicates that in control cells (siFF), the half-life of Cyclin F was approximately 137 minutes, consistent with prior observations (Choudhury et al., 2016; D'Angiolella et al., 2012). Following AKT depletion the half-life of Cyclin F was reduced to ~111 minutes (Figure 2C and 2D). Importantly, this decrease was not due to a gross change in cell cycle since the abundance of Cyclin A was unchanged between control and AKT depleted cells.

Cyclin F stability was next analyzed following acute, pharmacological AKT inactivation. Inhibiting AKT with afuresertib for 1.5 hours prior to the addition of CHX reduced endogenous Cyclin F half-life by 50 minutes (Figure 2E and 2F). Cyclin A levels were unchanged between DMSO and AKT inhibitor treated cells, indicating that changes in Cyclin F stability were not the result of cell cycle arrest. We performed a similar assay, analyzing endogenous Cyclin F stability in U2OS cells that were first synchronized in S-phase using an thymidine block and release protocol (Wang et al., 2017). Consistently, pharmacological AKT inactivation shortened Cyclin F half-life (Supplemental Figure 3A and B).

Finally, we examined Cyclin F stability following expression of constitutively active HA-Myr-AKT1. Ectopic expression of AKT1 increased the abundance and stability of Myc-Cyclin F being expressed from a heterologous promoter (Figure 2G and 2H), ruling out the possibility that changes in transcription account for its differential abundance and stability. Similarly, Cyclin A levels were unchanged between control and HA-Myr-AKT1 expressing cells, indicating that the cell cycle was not perturbed under these conditions. These data demonstrate an important role of AKT in controlling Cyclin F stability.

The ability of AKT to control Cyclin F stability (Figure 2), and to phosphorylate it on evolutionarily conserved consensus motifs (Figure 1), suggested that AKT might control Cyclin F through direct phosphorylation. We therefore compared the stability of Cyclin F^{WT} and a phospho-deficient mutant version where both AKT phosphorylation sites are changed to alanine (T31A, S577A; Cyclin F^{AA}). Importantly, Cyclin F^{AA} was significantly less stable than Cyclin F^{WT} (Figure 3A and 3B). Taken together, we conclude that direct AKT phosphorylation increases Cyclin F stability.

The first AKT consensus motif in Cyclin F (T31) is located in the F-box domain. The F-box domain connects substrate receptor F-box proteins to the ubiquitin machinery through a direct interaction with Skp1. We used *in silico* modeling predictions to examine the Cyclin F-Skp1 interaction. We modeled a segment of the F-box domain from Cyclin F into the previously annotated structure of Skp1-Fbxl3 (Xing et al., 2013). This analysis suggested that Cyclin F phosphorylation would increase Skp1 binding by introducing electrostatic interactions between Skp1 and Cyclin F (Figure 3C). In accordance with the *in silico* modeling, ectopic expression of HA-Myr-AKT1 significantly enhanced Cyclin F binding to Skp1 by co-IP (Figure 3D). To determine if AKT1 directly enhances binding between Cyclin F and Skp1, we examined binding using phospho-deficient and phospho-mimetic versions of Cyclin F (Cyclin F^{AA} and Cyclin F^{DD}). Importantly, Cyclin F^{DD} precipitated more Skp1 and Nedd8 modified Cul1, than Cyclin F^{AA} (Figure 3E). This is significant since Cul1 is Nedd8 conjugated in active SCF complexes (Duda et al., 2008; Saha and Deshaies, 2008). Similarly, Cyclin F^{DD} precipitated more Skp1 than Cyclin F^{WT}, whereas Cyclin F^{AA} precipitated less Skp1 (Figure 3F). These data indicate that AKT phosphorylation of Cyclin F increases SKP1 binding, enhancing its assembly into productive SCF ligase complexes.

When serum is withdrawn from HCT116 colon cancer cells and then added back to re-stimulate mitogen sensing pathways, we observed the expected increase in AKT activity, based on accumulation of phospho-Ser473 on AKT as well as phosphorylation of its substrate, GSK3β (Figure 4A). Likewise, there is a steady increase in Cyclin F abundance, starting as early as one hour after re-stimulation and continuing throughout a six-hour time course (Figure 4A). Cyclin A levels remained unchanged under these conditions, indicating that the transient withdrawal of serum did not interfere with the cell cycle. Consistently, pharmacological inhibition of signaling through the PI3K-AKT cascade for six hours with either LY294003 or AZD5363 (PI3K and AKT inhibitors, respectively) produced a significant reduction in Cyclin F protein levels (Figure 4B).

We recently demonstrated that SCF(Cyclin F) and APC/C(Cdh1) form a reciprocal circuit that contributes to cell cycle progression (Choudhury et al., 2016). Since AKT stabilizes Cyclin F and enhances its binding to Skp1-Cul1, we reasoned that AKT could modulate the Cyclin F-Cdh1 circuit. We first determined if AKT can enhance the degradation of Cdh1. Consistent with this notion, pharmacological inhibition of the PI3K-AKT cascade also increased Cdh1 levels (Figure 4B).

We established co-expression conditions where Cyclin F is efficiently degraded by Cdh1. This was achieved by co-expressing Myc-Cyclin F and FLAG-Cdh1, with the latter in excess (Figure 4C, lanes 1 vs 2). Remarkably, the addition of HA-Myr-AKT1 reversed the degradation reaction. When Cdh1, Cyclin F, and AKT1 are co-expressed (with Cdh1 in excess of Cyclin F), Cdh1 levels were reduced to nearly undetectable levels and Cyclin F was significantly increased, consistent with AKT stabilizing Cyclin F and destabilizing Cdh1 (Figure 4C, lanes 2 vs 4). Increasing the amount of AKT1 in this reaction further reduced Cdh1 levels, from very low to undetectable levels (Figure 4C, lane 4 vs 5). Consistently, ectopic expression of HA-Myr-AKT1 resulted in a dose-dependent degradation in Cdh1 (Supplemental Figure 4A).

To confirm that AKT is inducing Cdh1 ubiquitylation, we introduced HA-Myr-AKT1 into cells expressing hexa-histidine tagged ubiquitin. Cells were lysed under denaturing conditions and ubiquitylated proteins were captured on nickel agarose and analyzed by immunoblot. Under these conditions, AKT1 enhanced the ubiquitylation of endogenous Cdh1 (Figure 4D). Finally, we analyzed Cdh1 stability in a CHX chase experiment in cells expressing either Cyclin F^{WT} or the phospho-mimetic version, Cyclin F^{DD}. Consistently, Cdh1 half-life was reduced from 83 minutes to 50 minutes in Cyclin F^{DD} expressing cells (Supplementary Fig 4B and 4C) compared to Cyclin F^{WT} controls. We therefore conclude that AKT phosphorylation of Cyclin F enhances assembly of the SCF(Cyclin F) complex and contributes to the ubiquitylation and degradation Cdh1.

Cyclin F phosphorylation contributes to cell cycle progression

Despite the importance of AKT in cell cycle progression, the direct cell cycle targets of AKT remain largely unknown (Manning and Toker, 2017; Skeen et al., 2006). Since Cyclin F regulates cell cycle progression, we tested the importance of its AKT dependent phosphorylation. We synchronized non-transformed RPE1 cells in G0/G1 by serum deprivation for 24 hours. After serum refeeding followed by EdU labeling (to monitor S-phase entry), cells were fixed and stained on-plate for EdU incorporation using click-chemistry and for DNA using Hoechst. Most cells began DNA synthesis by 18 hours, based on EdU labeling (Figure 5A). Consistent with our prior report, depletion of Cyclin F reduced S-phase entry at 18 hours after re-feeding (Figure 5B).

To confirm the importance of AKT in cell cycle entry, we synchronized cells in G0/G1, released them into inhibitor treated, serum containing media, and monitored the percent of S-phase cells at 18 hours after release. The start of DNA replication was impaired by AKT inhibition (Afuresertib/GSK2110183), CRL and SCF ligase inactivation (MLN4924, neddylation inhibitor), proteasome inhibition (bortezomib), and CDK4/6 inhibition (Palbociclib/PD0332991) (Supplemental Figure 5A). Similar results were obtained with a second AKT inhibitor (Uprosertib/GSK2141795; data not shown). Similar to the need for proteasome activity and cullin-RING E3 ubiquitin ligases, these data highlight the importance of AKT activity in promoting S-phase entry, as has been described by others (Skeen et al., 2006).

We next examined the role of Cyclin F phosphorylation by AKT. RPE1 cells transiently overexpressing Cyclin F^{WT}, Cyclin F^{AA}, Cyclin F^{DD} or empty vector controls were serum starved and then re-fed to initiate cell cycle progression, monitoring S-phase entry by EdU incorporation. Immunoblots show that all three proteins were expressed at similar levels prior to refeeding (Figure 5C), consistent with the observations above that mitogen signaling is a significant determinant of Cyclin F abundance and stability. Cyclin F^{WT} and Cyclin F^{DD} enhanced the rate of S-phase entry compared to empty vector (Figure 5D and 5E). Significantly, S-phase entry was reduced in Cyclin F^{AA} expressing cells, relative to Cyclin F^{WT} and Cyclin F^{DD}. This demonstrates an important cell cycle function for Cyclin F phosphorylation by AKT.

The above experiments show that AKT phosphorylation of Cyclin F accelerates progress into S-phase from a G0/G1 arrest. However, rapid cell cycle entry can ultimately reduce

proliferation by causing damage during DNA replication. Notably, cells lacking Cdh1 rapidly progress through G1 phase (Choudhury et al., 2016; Sigl et al., 2009; Yuan et al., 2014) and accumulate DNA damage, based on staining for the damage marker γH2AX, and consistent with prior reports (Supplemental Figure 5B) (Bassermann et al., 2008; Choudhury et al., 2016; Engelbert et al., 2008; Sigl et al., 2009). We therefore tested the effect of longer-term expression of the various mutant versions of Cyclin F in HCT116 cells. Analysis of DNA content by flow cytometry showed that expression of Cyclin F^{DD} decreased the population of G2/M cells and increased the percent of G1 cells (Supplementary Figure 5C and 5D). This was accompanied by the accumulation of phosphorylated RB (Supplementary Figure 5E). Furthermore, Cyclin F^{DD} expressing cells accumulated phosphorylated Chk1, a marker of DNA damage induction (Supplementary Figure 5E). Together, these data point to an important role for AKT phosphorylation of Cyclin F in cell cycle progression and genome maintenance.

DISCUSSION

Cells mobilize intracellular signaling cascades to translate information from their extracellular environment into cellular responses and phenotypes. Pioneering studies demonstrated that cells sense the availability of nutrients, mitogens, and growth factors to pass through a restriction point in G1 phase and proceed into the cell cycle (Pardee, 1974; Zetterberg and Larsson, 1985). However, a molecular description of how cells transmit the presence of mitogens to the cell cycle machinery remains unclear. The most well-established connection between mitogen signaling pathways and the core cell cycle oscillator centers on the CDK4/6-RB-E2F pathway (Weinberg, 1995). In response to growth factors, cells upregulate transcription of Cyclin D, the activating subunit for the G1-phase CDK4/6 kinases (Peeper et al., 1997). CDK4/6 inactivates RB, enabling E2F-dependent transcription of myriad cell cycle genes and coupling extracellular cues to the cell cycle. Importantly, cells that are deficient in Cyclin D or CDK4/6 arrest when serum is withdrawn and re-enter the cell cycle upon refeeding (Kozar et al., 2004; Malumbres et al., 2004). This implies that other molecules and pathways are involved in connecting mitogen and nutrient sensing pathways to the core cell cycle machinery.

The APC/C is active throughout G1 and inhibited in S-phase. APC/C inactivation prior to G1/S represents a so-called “commitment point” for cell cycle entry (Brandeis and Hunt, 1996; Cappell et al., 2016). We recently showed that Cyclin F is targeted for degradation by the APC/C (Choudhury et al., 2016). Furthermore, we demonstrated that SCF(Cyclin F) is important for timely progression into S-phase due to its role in targeting Cdh1 for degradation in late G1 and S-phase (Choudhury et al., 2016).

Here we demonstrate that Cyclin F is a direct substrate of the oncogenic, cell cycle regulated kinase AKT. We show that AKT increases Cyclin F stability and enhances its assembly into SCF ligase complexes. The activation of AKT during the cell cycle and the consequent stabilization of Cyclin F do not appear precisely coordinated suggesting the AKT may control numerous other substrates, and that the ordering of these substrates might be highly regulated, as is the case for CDK targets (Swaffer et al., 2016). Our data are consistent with a model where AKT toggles a switch between Cyclin F-mediated Cdh1 degradation and

Cdh1 mediated Cyclin F degradation. APC/C(Cdh1) is a core component of the cell cycle oscillator due to its direct role in targeting mitotic Cyclins, among many other cell cycle proteins. Therefore, our data connect growth factor signaling through AKT to the core cell cycle oscillator via the F-box protein Cyclin F.

We propose a speculative model that a positive feedback loop, initiated by growth factor signaling and transmitted through AKT, helps to coordinate cell cycle progression. In this loop, AKT phosphorylates Cyclin F, enhancing its assembly into competent ligase complexes (above). SCF(Cyclin F) catalyzes the degradation of Cdh1, which otherwise restricts S-phase entry (Choudhury et al., 2016). With APC/C activity disabled via Cdh1 destruction (and likely through additional mechanisms), Cyclin A accumulates and activities CDK2, amplifying the loop through positive feedback. This positive feedback comes from the ability Cyclin A-Cdk2 to activate AKT (Liu et al., 2014), and because Cyclin A-CDK2 dependent phosphorylation of Cdh1 impairs its binding to the APC/C core complex, further restraining APC/C activity (Lukas et al., 1999). The inactivation of both AKT and CDK in late mitosis resets the system. Evaluating this model with computational and experimental analysis is an important future question. This model has potential implications regarding the mechanism by which cells arrest in response to growth factor withdrawal (Pardee, 1974).

We have also demonstrated a unique mechanism for regulating substrate ubiquitylation and degradation, namely, the phospho-dependent assembly of a CRL-type E3 ligase complex. We found that AKT phosphorylation of Cyclin F enhances its assembly into functional ligase complexes. However, the structural features in Cyclin F that increase binding to Skp1 remain unclear. Dissecting the relative contributions of the two AKT phosphorylation sites to Skp1 binding remains an important question. Determining the structure of the Cyclin F-Skp1 complex will shed light on the mechanisms of SCF assembly and their regulation of phosphorylation.

It has previously been established that phosphorylation, as well as other post-translational modifications of substrates, plays an important role in regulating ligase-substrate interactions. This places the point of regulation for SCF substrate ubiquitylation at the level of the substrate. However, there are alternative mechanisms that control substrate ubiquitylation for non-SCF E3 ligases. For example, for the APC/C, substrate modification is controlled at the ligase level, which is turned on or off through myriad mechanisms. One such mechanism regulates the ability of the APC/C substrate receptor Cdh1 to associate with the E3 via phosphorylation, thereby controlling substrate degradation. We show here that phosphorylation controls the assembly of SCF(Cyclin F) ligases. This raises the possibility that assembly and activation of additional SCF complexes is controlled in a similar fashion. Moreover, these data suggest the intriguing possibility that the global allocation of F-box proteins into competent E3 ligase complexes is dynamically controlled by phospho-signaling cascades. The conservation of phosphorylation sites at and nearby to the same site as T31 in other F-box proteins support this idea. We predict that coupling ligase assembly to signal transduction regulators that sense the physiological state of the cell could allow for the dynamic reorganization of the assembled E3 ligase repertoire.

The G1/S boundary is a common target of oncogenic perturbation. For example, inactivating mutations in the retinoblastoma tumor suppressor are common in many cancers. Cdh1 is important in controlling G1, and loss of a single allele in mice can cause cancer (García-Higuera et al., 2008). However, Cdh1 is neither mutated nor deleted in human malignancies. Thus, it remains unclear if Cdh1 is inactivated in human cancer. Our discovery that activated AKT can post-translationally repress Cdh1 suggests that cancers with activated AKT are likely to have reduced APC/C(Cdh1) activity at the G1/S boundary. This mechanism would obviate the need to genetically inactivate Cdh1, which increases DNA damage and could be cell lethal. Reports in flies, worms, and human cells have indicated that Cdh1 and the CDK4/6-RB pathway cooperate in controlling cell cycle entry (Binné et al., 2007; Buttitta et al., 2010; Fay et al., 2002; The et al., 2015). These observations, and our demonstration that AKT represses Cdh1, indicate a potential explanation for the synergy observed between PI3K and CDK4/6 inhibitors in models of breast cancer (Vora et al., 2014).

EXPERIMENTAL PROCEDURES

Mammalian cell culture and immunoblotting

HEK-293T, HCT-116, RPE1, HeLa and U2OS cells were obtained from ATCC, and grown in DMEM complete medium (Gibco) supplemented with 10% fetal bovine serum (Atlanta Biologicals). The small molecule inhibitors of AKT (AZD5363 and GSK-2141795) and PI3K (LY94002) were purchased from Selleckchem and added to cells for 6 hours at a final concentration of 10μM each. Prior to cycloheximide chase, 10μM AKT inhibitor (GSK-2141795) was added for 6 hours and chase and was performed in presence of the inhibitor.

Transfection experiments were performed in HEK-293T or HCT-116 cells unless otherwise stated. Cell lysis for immunoblot and SDS-PAGE is performed using standard techniques, as described in the supplemental experimental procedures.

Molecular biology

Cyclin F constructs were generated as mentioned previously (Choudhury et al., 2016). All genes were subcloned using PCR, and mutants generated using site directed mutagenesis were sequence verified. PCR amplification of DNA was performed using Hi fidelity DNA polymerase purchased from New England Biolabs or Agilent Inc. Myc tagged Cyclin F vectors were mutated using standard site directed mutation protocols. FLAG-Cyclin F truncation constructs were gift from Michele Pagano. The HA tagged version of HA-Myr-AKT was a gift from Dr. Channing Der.

All siRNA transfection experiments were performed using RNAimax (Life Technologies). The oligonucleotide sequences for siRNA used in this study are detailed in the key resources table. The sequences for siRNAs are available in the supplemental experimental procedures.

Immuno-precipitation

Standard procedures of immuno-precipitation (IP) were used. Myc tagged Cyclin F WT or mutants in HEK 293T cells for 24 h. FLAG-tagged full length Cyclin F or truncated versions

were co-expressed Myr-HA AKT. Cells were dislodged by trypsinization, washed with PBS (DIFCO) and lysed in NETN for 30 min at 4°C with occasional vortexing. Cell debris were removed by centrifugation at 15,000 rpm for 15 min at 4°C. Anti-FLAG M2, anti-HA or anti-Myc beads (20 ml per IP, Sigma, Cat No F2426, E6779 and E6654 respectively) were equilibrated on a rotary shaker in lysis buffer. The clarified lysate was loaded on the beads and bound on rotary shaker for 4h to overnight at 4°C. The beads were washed with lysis buffer three times and then incubated with sample buffer (60 mM Tris pH 6.8, 2% SDS, 10% glycerol, 100 mM DTT and 0.1% Bromophenol Blue) at 70°C for 10 minutes. For purification of Myc-Cyclin F^{WT} or Myc-Cyclin F^{AA} used in in vitro kinase assays, mutant cells expressing these constructs were lysed in NETN buffer without phosphatase inhibitor, immunoprecipitated with anti-Myc beads, and eluted using 100 mM Glycine (pH 2.0). Eluents were neutralized with 1M Tris base to pH 7.5.

Endogenous Cyclin F IP was performed from extracts obtained from HEK-293T. Briefly, cells are lysed in NETN lysis buffer for 30 min at 4°C an d clarified using centrifugation. Lysates were mixed with 1μg of the Cyclin F polyclonal Rabbit antibody (sc-952) and 75μl of the equilibrated protein A/G beads. Control beads were prepared using normal Rabbit IgG (sc-2027). Lysate, antibody and bead slurry was incubated at 4°C in rotary agitator over night washed three times with NETN lysis buffer and eluted as above.

Mass spectrometry analysis

Samples were prepared from cell expressing Myc-Cyclin F with and without HA-Myr-AKT1. Myc-Cyclin F was immunoprecipitated and subjected to SDS-PAGE and stained with coomassie. The bands corresponding to Cyclin F were excised and the proteins were reduced, alkylated, and in-gel digested with trypsin overnight at 37°C. The extracted peptides were enriched for phosphopeptides with IMAC as previously described (Chien et al., 2011). The bound peptides were eluted with 5% NH_4OH from IMAC resin, then acidified, dried via vacuum centrifugation and stored at −80°C until analysis. Detailed description of LC-MS/MS is available in the supplemental experimental procedures.

In vitro kinase Assay

Myc-Cyclin F WT or AA protein was purified from 293T cells as described above and subject to *in vitro* kinase assay. GST-AKT1 was purchased form Sigma (Figure 1; Cat# SRP 5001). Purified HA-Myr-AKT1 was isolated by pulldown from HEK293T cells (Supplemental Figure 1) as described (Liu et al., 2014). Kinase assays were performed in kinase buffer (25 mM MOPS, pH 7.2, 12.5 mM glycerol 2–phosphate, 25 mM $MgCl_2$, 5 mM EGTA, 2 mM EDTA and 0.25 mM DTT). The reaction was initiated with addition of ATP (1 μM) and performed at 30°C for 15–20 min and terminated by addition of sample buffer. The experiments in Figure 1 were carried out using recombinant GST-AKT1 and were analyzed using HA-Myr-Akt1 an AKT phospho motif antibody. The experiments in Supplemental Figure 1 were carried out using HA-Myr-AKT1 and analyzed using autoradiography for incorporation of [γ-32P] as previously described (Liu et al., 2014).

In vivo ubiquitination and isolation of 6His-Ubiquitinated proteins

HEK-293T cells were transfected using Lipofectamine 2000 in 10 cm dishes and harvested in Phosphate Buffer Saline 24 h post-transfection. A FLAG-HIS ubiquitin construct (6-His-Flag-Ub) was used for these studies, and was a generous gift from Dr. Philippe Soubeyran. 80% of the cell suspension was lysed in buffer 1 [6 M Guanidine-HCl, 0.1 M Na_2HPO_4/NaH_2PO_4, 0.01 M Tris/HCl, pH 8.0, 15 mM imidazole and 10 mM β-mercaptoethanol (βME)] and was used for pulldown of HIS-ubiquitin conjugated proteins. The remaining 20% of the cell suspension was used to prepare whole cell extracts and to analyze inputs by immunoblot. The lystates used for pulldown were sonicated to reduce viscosity, and loaded onto 50 μl of Ni^{2+}-NTA resin (Thermo Scientific) pre-washed with buffer 1. Binding of the His tagged ubiquitin was performed at room temperature (RT) for 4 h. The beads were successively washed with 750 μl of each of the following buffers: buffer 1; buffer 2 (8 M Urea, 0.1 M Na_2HPO_4/NaH_2PO_4, 0.01 M Tris/HCl, pH 8.0, 10 mM βME); buffer 3 (8 M Urea, 0.1 M Na_2HPO_4/NaH_2PO_4, 0.01 M Tris/HCl, pH 6.3, 10mM βME) plus 0.2% Triton X-100; buffer 3 and then buffer 3 plus 0.1% Triton X-100. After the last wash, bound proteins were eluted by incubating the beads in 50 μl of buffer 4 (200 mM imidazole, 0.15 M Tris/HCl pH 6.7, 30% glycerol, 0.72 M βME, 5% SDS) for 20 min at RT. Eluates were analyzed by immunoblot.

Flow Cytometry and on plate EDU incorporation analysis

For flow cytometry analysis was in HCT116 cells were fixed in 70% ethanol and stained with propidium iodide using standard methods. Flow cytometry analysis was performed on CyAn ADP Analyzer. Non-transformed RPE1 cells were transfected using Lipofectamine 3000 and serum starved for 24 hours to synchronize cells in G0/G1. Serum was added back to promote S-phase which was monitored by EdU (5-Ethynyl-2′-deoxyuridine; Sigma # T511285) incorporation. Cells were fixed on plates in 3.7% formaldehyde and washed in PBS prior to EdU labeling by azide-alkyne cycloaddition click chemistry. Click reactions are a total of 500 μl in PBS, and include: Alexa Fluor 488 Azide (final concentration of 1 μM), CuSO4 (final concentration of 1mM), ascorbic acid (final concentration of 100mM. The labeled cells were counter stained for DNA with 7-AAD or Hoechst. RPE-1 cells were plated in triplicate in 96-well plates at 5,000 cells/well and allowed to attach overnight. Cells were washed twice briefly in 1× PBS, synchronized in serum-free medium for 24 hr. G0 synchronized cells were then simultaneously released into cell cycle with medium containing 10% fetal bovine serum in the presence of 10μM EdU and treated with increasing concentrations of the inhibitor (Afuresertib, MLN4924, Boterzomib, or Palbociclib) or vehicle (DMSO) for 18 hr. Cells were subsequently stained with the fluorescent azide as mentioned above. Images were captured on an EVOS™ FL Auto Imaging System (Life Technologies) and processed in ImageJ to obtain the percentage of EdU positive S-phase cells within the total number of cells in the field.

Homology based protein modeling

The HHpred server (http://toolkit.tuebingen.mpg.de/hhpred) was used to identify suitable structural templates for building a model of the Cyclin F/Skp1 complex (Soding, 2005). A model of the Cyclin F/Skp1 complex was built based on the structure of Fbxl3/Skp1 (PDB

ID: 4I6J) using Modeller 9.15 (Eswar et al., 2007). A rotamer was selected for the side chain of lysine 142 of Skp1 and a dihedral angle was selected for the phosphothreonine of Cyclin F that optimized the potential for an electrostatic interaction between the two residues.

Supplementary Material

Refer to Web version on PubMed Central for supplementary material.

Acknowledgments

Special thanks to the Emanuele laboratory for feedback throughout this study. We thank the following individuals for providing reagents: Channing Der (UNC, Chapel Hill), Peter Jackson (Stanford University), and Philippe Soubeyran (Institut Paoli-Calmettes, Aix-Marseille Université). Thanks to Dr. Brenda R. S. Temple (UNC Structural Bioinformatics Core Facility) for molecular modeling assistance. This work was done in part with the UNC Flow Cytometry and Proteomics Core Facilities, which are supported in part by P30 CA016086 Cancer Center Core Support Grant to the Lineberger Cancer Center. This work was supported by start-up funds from the University Cancer Research Fund, and grants from the Susan G. Komen Foundation (CCR14298820), Jimmy-V Foundation, and National Institute of Health (R01GM120309) (MJE, RC, TB, AA, XW, JLK, and CAM). CAM and JLK were supported by a pre-doctoral T32 training grant to the UNC Department of Pharmacology.

References

Bai C, Sen P, Hofmann K, Ma L, Goebl M, Harper JW, Elledge SJ. SKP1 connects cell cycle regulators to the ubiquitin proteolysis machinery through a novel motif, the F-box. Cell. 1996; 86:263–274. [PubMed: 8706131]

Bassermann F, Frescas D, Guardavaccaro D, Busino L, Peschiaroli A, Pagano M. The Cdc14B-Cdh1-Plk1 axis controls the G2 DNA-damage-response checkpoint. Cell. 2008; 134:256–267. [PubMed: 18662541]

Binné UK, Classon MK, Dick Fa, Wei W, Rape M, Kaelin WG, Näär AM, Dyson NJ. Retinoblastoma protein and anaphase-promoting complex physically interact and functionally cooperate during cell-cycle exit. Nat Cell Biol. 2007; 9:225–232. [PubMed: 17187060]

Brandeis M, Hunt T. The proteolysis of mitotic cyclins in mammalian cells persists from the end of mitosis until the onset of S phase. EMBO J. 1996; 15:5280–5289. [PubMed: 8895573]

Buttitta LA, Katzaroff AJ, Edgar BA. A robust cell cycle control mechanism limits E2F-induced proliferation of terminally differentiated cells in vivo. J Cell Biol. 2010; 189:981–996. [PubMed: 20548101]

Cappell SD, Chung M, Jaimovich A, Spencer SL, Meyer T. Irreversible APCCdh1 Inactivation Underlies the Point of No Return for Cell-Cycle Entry. Cell. 2016; 166:167–180. [PubMed: 27368103]

Chien KY, Liu HC, Goshe MB. Development and application of a phosphoproteomic method using electrostatic repulsion-hydrophilic interaction chromatography (ERLIC), IMAC, and LC-MS/MS analysis to study Marek's disease virus infection. J Proteome Res. 2011; 10:4041–4053. [PubMed: 21736374]

Choudhury R, Bonacci T, Arceci A, Lahiri D, Mills CA, Kernan JL, Branigan TB, DeCaprio JA, Burke DJ, Emanuele MJ. APC/C and SCF(cyclin F) Constitute a Reciprocal Feedback Circuit Controlling S-Phase Entry. Cell Rep. 2016; 16:3359–3372. [PubMed: 27653696]

D'Angiolella V, Donato V, Vijayakumar S, Saraf A, Florens L, Washburn MP, Dynlacht B, Pagano M. SCF Cyclin F controls centrosome homeostasis and mitotic fidelity through CP110 degradation. Nature. 2010; 466:138–142. [PubMed: 20596027]

D'Angiolella V, Donato V, Forrester FM, Jeong Y, Pellacani C, Kudo Y, Saraf A, Florens L, Washburn MP, Pagano M. Cyclin F-Mediated Degradation of Ribonucleotide Reductase M2 Controls Genome Integrity and DNA Repair. Cell. 2012; 149:1023–1034. [PubMed: 22632967]

D'Angiolella V, Esencay M, Pagano M. A cyclin without cyclin-dependent kinases: cyclin F controls genome stability through ubiquitin-mediated proteolysis. Trends Cell Biol. 2013; 23:135–140. [PubMed: 23182110]

Dephoure N, Gould KL, Gygi SP, Kellogg DR. Mapping and analysis of phosphorylation sites: a quick guide for cell biologists. Mol Biol Cell. 2013; 24:535–542. [PubMed: 23447708]

Duda DM, Borg LA, Scott DC, Hunt HW, Hammel M, Schulman BA. Structural Insights into NEDD8 Activation of Cullin-RING Ligases : Conformational Control of Conjugation. Cell. 2008; 1:995–1006.

Elia AEH, Boardman AP, Wang DC, Huttlin EL, Everley RA, Dephoure N, Zhou C, Koren I, Gygi SP, Elledge SJ. Quantitative Proteomic Atlas of Ubiquitination and Acetylation in the DNA Damage Response. Mol Cell. 2015:1–15.

Emanuele MJ, Elia AEH, Xu Q, Thoma CR, Izhar L, Leng Y, Guo A, Chen YN, Rush J, Hsu PW, et al. Global identification of modular cullin-RING ligase substrates. Cell. 2011; 147:459–474. [PubMed: 21963094]

Engelbert D, Schnerch D, Baumgarten a, Wäsch R. The ubiquitin ligase APC(Cdh1) is required to maintain genome integrity in primary human cells. Oncogene. 2008; 27:907–917. [PubMed: 17700535]

Eswar N, Webb B, Marti-Renom Ma, Madhusudhan MS, Eramian D, Shen MY, Pieper U, Sali a. Comparative protein structure modeling using MODELLER. Curr Protoc Protein Sci. 2007 Chapter 2, Unit 2 9.

Fay DS, Keenan S, Han M. fzr-1 and lin-35/Rb function redundantly to control cell proliferation in C. elegans as revealed by a nonbiased synthetic screen. Genes Dev. 2002; 16:503–517. [PubMed: 11850412]

García-Higuera I, Manchado E, Dubus P, Cañamero M, Méndez J, Moreno S, Malumbres M. Genomic stability and tumour suppression by the APC/C cofactor Cdh1. Nat Cell Biol. 2008; 10:802–811. [PubMed: 18552834]

Hershko A, Ciechanover A. The ubiquitin system. Annu Rev Biochem. 1998; 67:425–479. [PubMed: 9759494]

Jin J, Cardozo T, Lovering RC, Elledge SJ, Pagano M, Harper JW. Systematic analysis and nomenclature of mammalian F-box proteins. 2004:2573–2580.

Kandel ES, Skeen J, Majewski N, Di Cristofano A, Pandolfi PP, Feliciano CS, Gartel A, Hay N. Activation of Akt / Protein Kinase B Overcomes a G 2 / M Cell Cycle Checkpoint Induced by DNA Damage. Mol Cell Biol. 2002; 22:7831. [PubMed: 12391152]

Kozar K, Ciemerych MA, Rebel VI, Shigematsu H, Zagozdzon A, Sicinska E, Geng Y, Yu Q, Bhattacharya S, Bronson RT, et al. Mouse development and cell proliferation in the absence of D-cyclins. Cell. 2004; 118:477–491. [PubMed: 15315760]

Liu P, Begley M, Michowski W, Inuzuka H, Ginzberg M, Gao D, Tsou P, Gan W, Papa A, Kim BM, et al. Cell-cycle-regulated activation of Akt kinase by phosphorylation at its carboxyl terminus. Nature. 2014

Lukas C, Sørensen CS, Kramer E, Santoni-Rugiu E, Lindeneg C, Peters JM, Bartek J, Lukas J. Accumulation of cyclin B1 requires E2F and cyclin-A-dependent rearrangement of the anaphase-promoting complex. Nature. 1999; 401:815–818. [PubMed: 10548110]

Malumbres M, Sotillo R, Santamaría D, Galán J, Cerezo A, Ortega S, Dubus P, Barbacid M. Mammalian cells cycle without the D-type cyclin-dependent kinases Cdk4 and Cdk6. Cell. 2004; 118:493–504. [PubMed: 15315761]

Manning BD, Toker A. AKT/PKB Signaling: Navigating the Network. Cell. 2017; 169:381–405. [PubMed: 28431241]

Manning BD, Logsdon MN, Lipovsky AI, Abbott D, Kwiatkowski DJ, Cantley LC. Feedback inhibition of Akt signaling limits the growth of tumors lacking Tsc2. Genes Dev. 2005; 19:1773–1778. [PubMed: 16027169]

Pardee AB. A Restriction Point for Control of Normal Animal Cell Proliferation. 1974; 71:1286–1290.

Peeper DS, Upton TM, Ladha MH, Neuman E, Zalvide J, Bernards R, DeCaprio JA, Ewen ME. Ras signalling linked to the cell-cycle machinery by the retinoblastoma protein. Nature. 1997; 386:177–181. [PubMed: 9062190]

Petroski MD, Deshaies RJ. Function and regulation of cullin-RING ubiquitin ligases. Nat Rev Mol Cell Biol. 2005; 6:9–20. [PubMed: 15688063]

Saha A, Deshaies RJ. Multimodal activation of the ubiquitin ligase SCF by Nedd8 conjugation. Mol Cell. 2008; 32:21–31. [PubMed: 18851830]

Shtivelman E, Sussman J, Stokoe D. A role for PI 3-kinase and PKB activity in the G2/M phase of the cell cycle. Curr Biol. 2002; 12:919–924. [PubMed: 12062056]

Sigl R, Wandke C, Rauch V, Kirk J, Hunt T, Geley S. Loss of the mammalian APC/C activator FZR1 shortens G1 and lengthens S phase but has little effect on exit from mitosis. J Cell Sci. 2009; 122:4208–4217. [PubMed: 19861496]

Skaar JR, Pagan JK, Pagano M. SCF ubiquitin ligase-targeted therapies. Nat Rev Drug Discov. 2014; 13:889–903. [PubMed: 25394868]

Skeen JE, Bhaskar PT, Chen CC, Chen WS, Peng X ding, Nogueira V, Hahn-Windgassen A, Kiyokawa H, Hay N. Akt deficiency impairs normal cell proliferation and suppresses oncogenesis in a p53-independent and mTORC1-dependent manner. Cancer Cell. 2006; 10:269–280. [PubMed: 17045205]

Soding J. Protein homology detection by HMM-HMM comparison. Bioinformatics. 2005; 21:951–960. [PubMed: 15531603]

Sørensen CS, Lukas C, Kramer ER, Peters J, Bartek J, Lukas J. A Conserved Cyclin-Binding Domain Determines Functional Interplay between Anaphase-Promoting Complex – Cdh1 and Cyclin A-Cdk2 during Cell Cycle Progression A Conserved Cyclin-Binding Domain Determines Functional Interplay between Anaphase-Promoting Comple. 2001

Swaffer MP, Jones AW, Flynn HR, Snijders AP, Nurse P. CDK Substrate Phosphorylation and Ordering the Cell Cycle. Cell. 2016; 167:1750–1761.e16. [PubMed: 27984725]

Temin HM. Stimulation by serum of multiplication of stationary chicken cells. J Cell Physiol. 1971; 78:161–170. [PubMed: 5167847]

Tetzlaff MT, Bai C, Finegold M, Harper JW, Mahon KA, Stephen J, Wilson J, Elledge SJ. Cyclin F Disruption Compromises Placental Development and Affects Normal Cell Cycle Execution. Mol Cell Biol. 2004; 24:2487–2498. [PubMed: 14993286]

The I, Ruijtenberg S, Bouchet BP, Cristobal A, Prinsen MBW, van Mourik T, Koreth J, Xu H, Heck AJR, Akhmanova A, et al. Rb and FZR1/Cdh1 determine CDK4/6-cyclin D requirement in C. elegans and human cancer cells. Nat Commun. 2015; 6:5906. [PubMed: 25562820]

Varshavsky A. The ubiquitin system, an immense realm. Annu Rev Biochem. 2012; 81:167–176. [PubMed: 22663079]

Vashisht AA, Zumbrennen KB, Huang X, Powers DN, Durazo A, Sun D, Bhaskaran N, Persson A, Uhlen M, Sangfelt O, et al. Control of iron homeostasis by an iron-regulated ubiquitin ligase. Science. 2009; 326:718–721. [PubMed: 19762596]

Vora SR, Juric D, Kim N, Mino-Kenudson M, Huynh T, Costa C, Lockerman EL, Pollack SF, Liu M, Li X, et al. CDK 4/6 Inhibitors Sensitize PIK3CA Mutant Breast Cancer to PI3K Inhibitors. Cancer Cell. 2014; 26:136–149. [PubMed: 25002028]

Walter D, Hoffmann S, Komseli ES, Rappsilber J, Gorgoulis V, Sørensen CS. SCFCyclin F-dependent degradation of CDC6 suppresses DNA re-replication. Nat Commun. 2016; 7:10530. [PubMed: 26818844]

Wang X, Arceci A, Bird K, Mills CA, Choudhury R, Kernan JL, Zhou C, Bae-Jump V, Bowers A, Emanuele MJ. VprBP/DCAF1 regulates the degradation and non-proteolytic activation of the cell cycle transcription factor FoxM1. Mol Cell Biol. 2017

Weinberg RA. The retinoblastoma protein and cell cycle control. Cell. 1995; 81:323–330. [PubMed: 7736585]

Xing W, Busino L, Hinds TR, Marionni ST, Saifee NH, Bush MF, Pagano M, Zheng N. SCF(FBXL3) ubiquitin ligase targets cryptochromes at their cofactor pocket. Nature. 2013; 496:64–68. [PubMed: 23503662]

Yuan X, Srividhya J, De Luca T, Lee JHE, Pomerening JR. Uncovering the role of APC-Cdh1 in generating the dynamics of S-phase onset. Mol Biol Cell. 2014; 25:441–456. [PubMed: 24356446]

Zachariae W. Control of Cyclin Ubiquitination by CDK-Regulated Binding of Hct1 to the Anaphase Promoting Complex. 1998; 282(80-):1721–1724.

Zetterberg, a, Larsson, O. Kinetic analysis of regulatory events in G1 leading to proliferation or quiescence of Swiss 3T3 cells. Proc Natl Acad Sci U S A. 1985; 82:5365–5369. [PubMed: 3860868]

Zheng N, Zhou Q, Wang Z, Wei W. Recent advances in SCF ubiquitin ligase complex: clinical implications. Biochim Biophys Acta. 2016; 1866:12–22. [PubMed: 27156687]

Highlights

- The cell cycle regulated F-box protein Cyclin F is an AKT substrate
- Phosphorylation by AKT increases Cyclin F stability
- Cyclin F phosphorylation promotes its assembly into E3 ligase complexes
- AKT phosphorylation of Cyclin F promotes the G1/S-phase transition

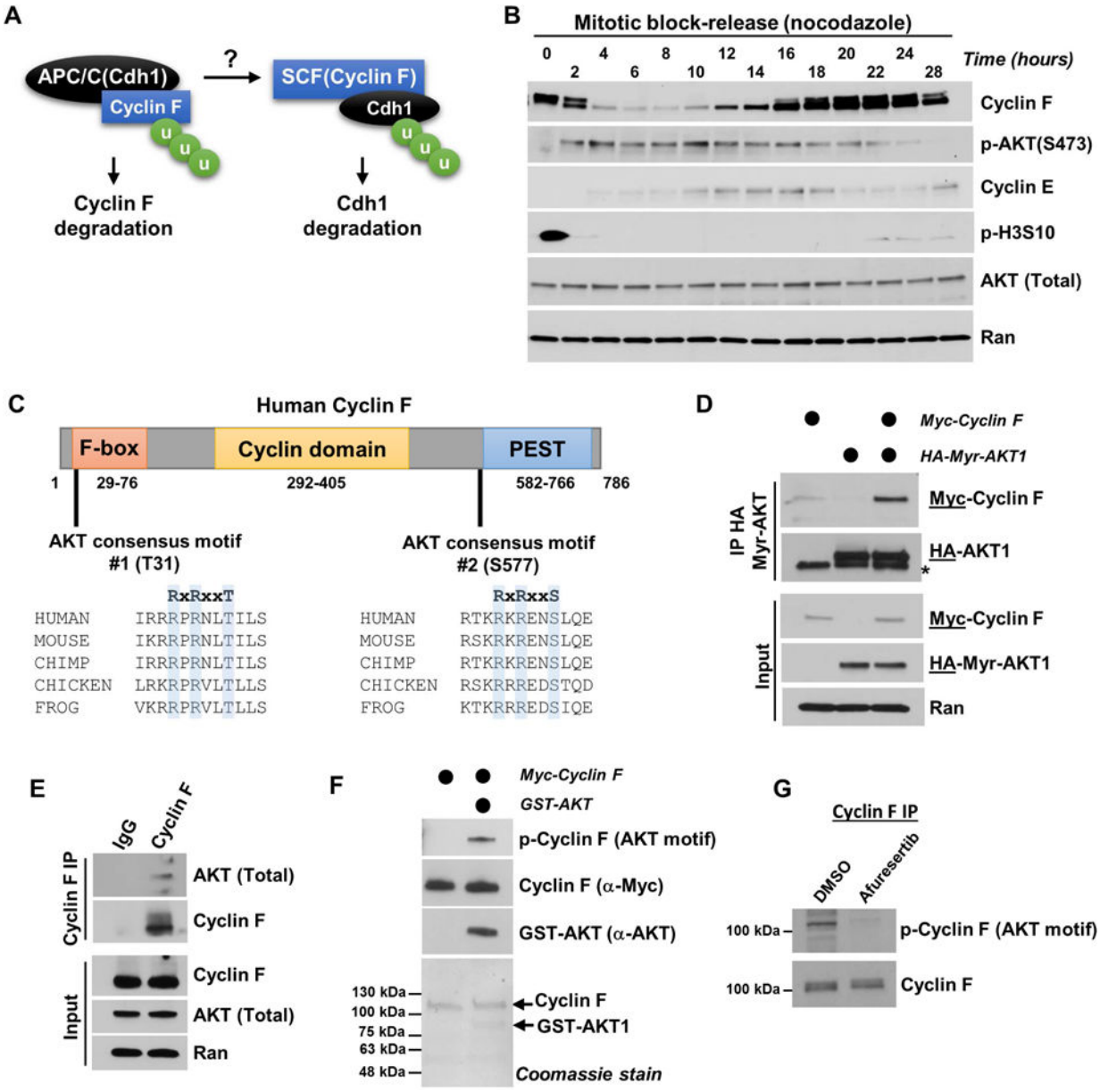

Figure 1. Cyclin F is an AKT substrate

(A) Schematic of the reciprocal, cell cycle dependent regulation of Cyclin F and Cdh1 by ubiquitination.

(B) U2OS cells were synchronized in mitosis with nocodazole, isolated by “shake-off”, and analyzed by immunoblot after release into the cell cycle.

(C) Domain structure of human Cyclin F showing the position of Cyclin homology, F-box and PEST domains, and two putative AKT phosphorylation sites. Conserved AKT sites are shown as multiple sequence alignments. The AKT consensus motifs are shaded in blue.

(D) Myr-HA-AKT1 and Myc-Cyclin F were ectopically expressed in 293T cells and immunoprecipitated on anti-HA beads. Asterisk indicates nonspecific band resulting from IgG. Immunoblotted antigen is underlined to the right of blots.

(E) Endogenous Cyclin F was immunoprecipitated from 293T cells and immunoblotted for AKT and Cyclin F.
(F) *In vitro* kinase assay was performed using recombinant GST-AKT1 and purified human Cyclin F. Phosphorylation was detected using an AKT phospho-motif specific antibody.
(G) Endogenous Cyclin F was immuno-precipitated from 293T cell extracts, washed stringently, and then probed with an AKT phospho-motif antibody. Prior to harvesting, cells were treated with an AKT inhibitor (afuresertib) or vehicle (DMSO) control.

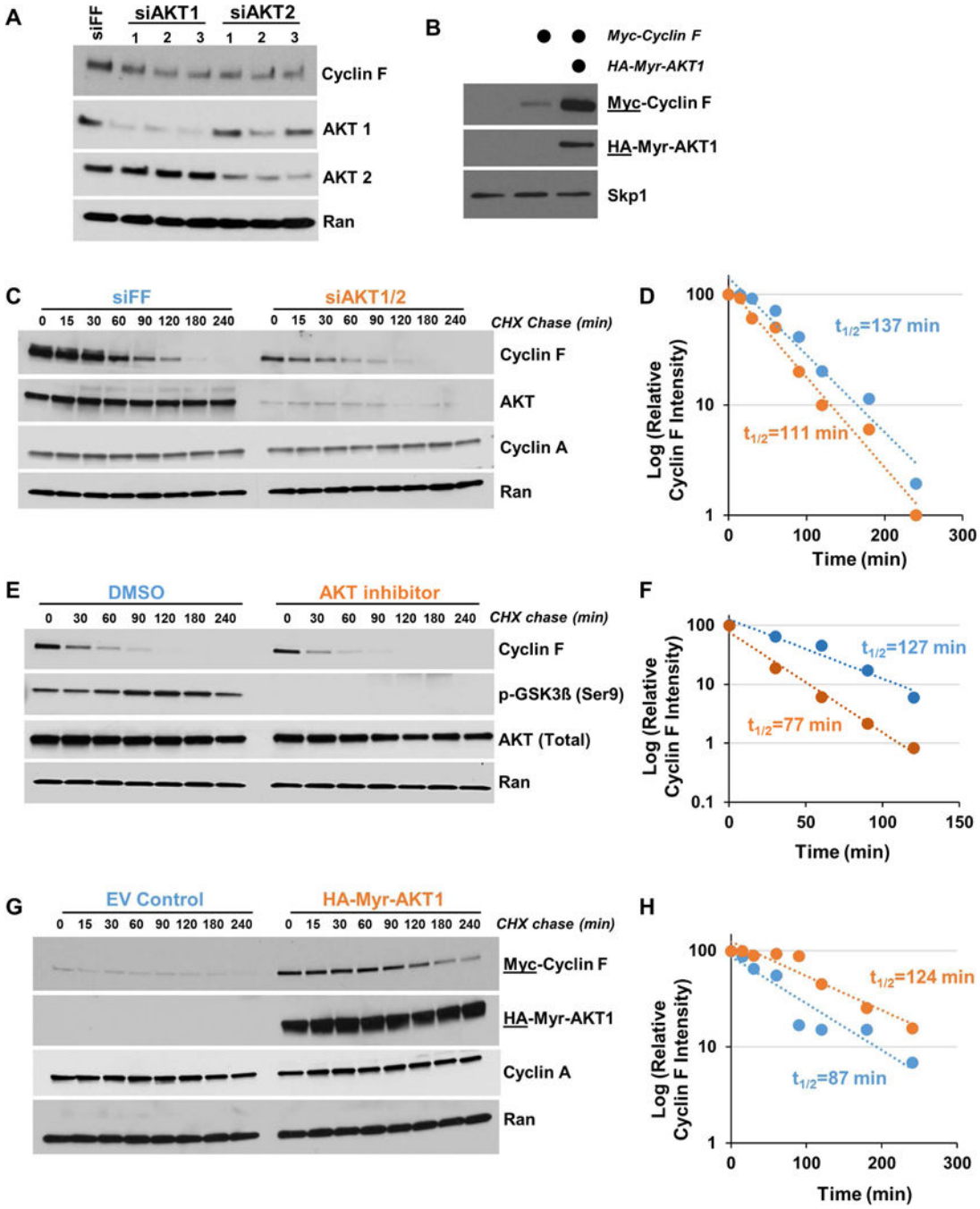

Figure 2. Cyclin F stability is regulated by the AKT activity

(A) Depletion of AKT1 or AKT2 in 293T cells with multiple siRNA reagents decreased Cyclin F abundance.

(B) Ectopic expression of AKT1 significantly increases the abundance of Myc-Cyclin F.

(C and D) Depletion of AKT1/2 decreases the half-life of endogenous Cyclin F in 293T cells.

(E and F) Pharmacological inhibition of AKT activity in HCT116 cells reduces the half-life of endogenous Cyclin F.

(G and H) Overexpression of constitutively active AKT (HA-Myr-AKT1) increases the half-life of ectopically expressed Myc-Cyclin F. In all immunoblot quantifications (*above-right*), blue indicates control and orange indicates experimental condition.

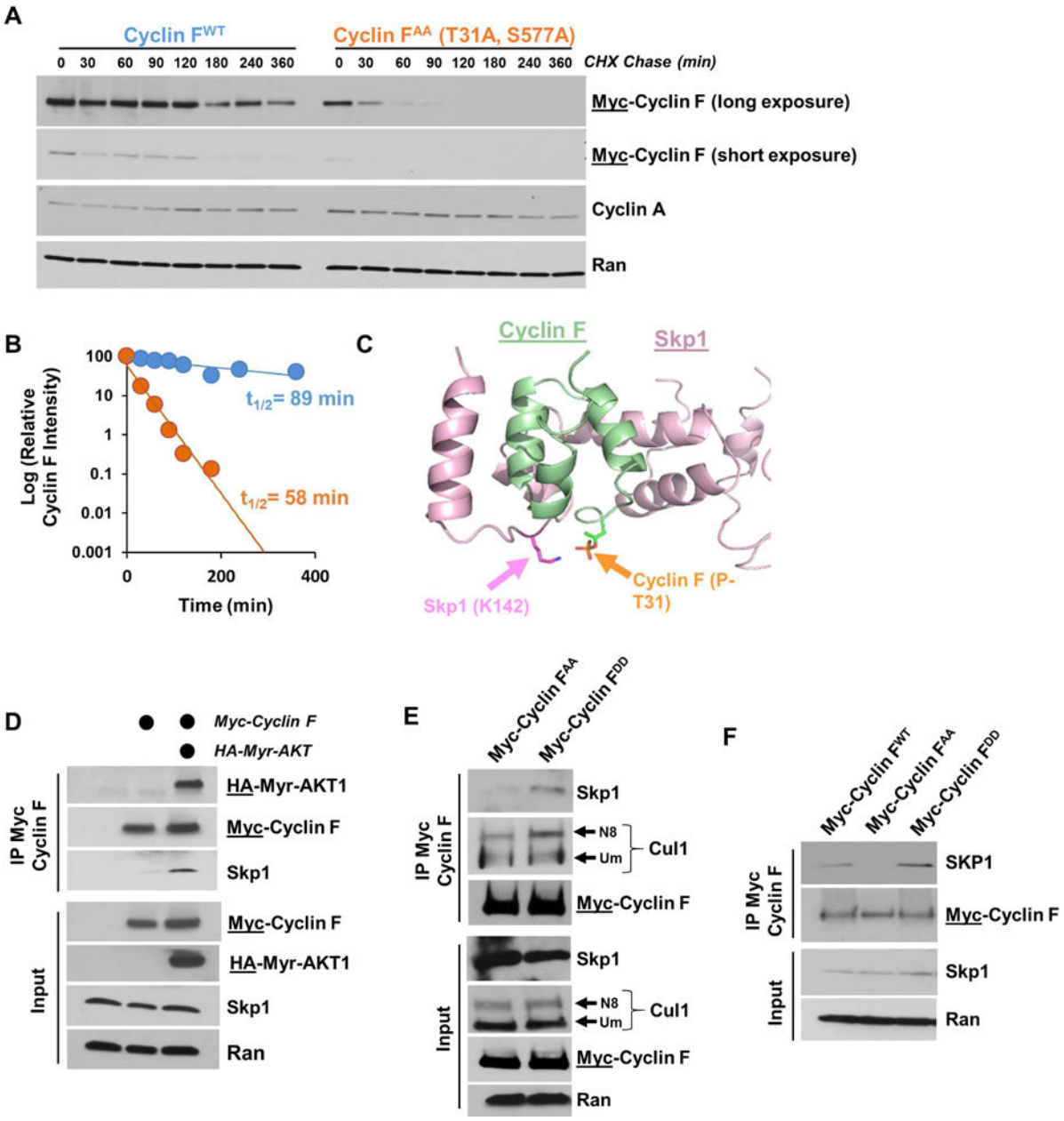

Figure 3. SCF(Cyclin F) assembly is regulated by AKT phosphorylation

(A) Stability analysis of Myc-Cyclin F^{WT} and Myc-Cyclin F^{AA} was performed in 293T cells by cycloheximide chase, indicating that Cyclin F^{AA} is unstable compared to Cyclin F^{WT}.

(B) Quantification of immunoblots shown in panel *A*.

(C) Cyclin F and Skp1 homology modelling predicts that phosphorylation of T31 in Cyclin F will introduce an electrostatic interaction with lysine 142 in Skp1, leading to better docking. Stick representations highlight the positions of K142 in Skp1 and phospho-T31 in Cyclin F.

(D) Ectopic expression of AKT increases Cyclin F-Skp1 biding based on anti-Myc Cyclin F coIP from 293T cells.

(E) Ectopic expression and immunoprecipitation of Myc-Cyclin F^{AA} (T31A, S577A) or Myc-Cyclin F^{DD} (T31D, S577D) in 293T cells leads to differential Skp1-Cul1-Cyclin F binding.

(F) Myc-Cyclin F^{WT} and phospho-mutant versions were precipitated from 293T cells and analyzed by immunoblot.

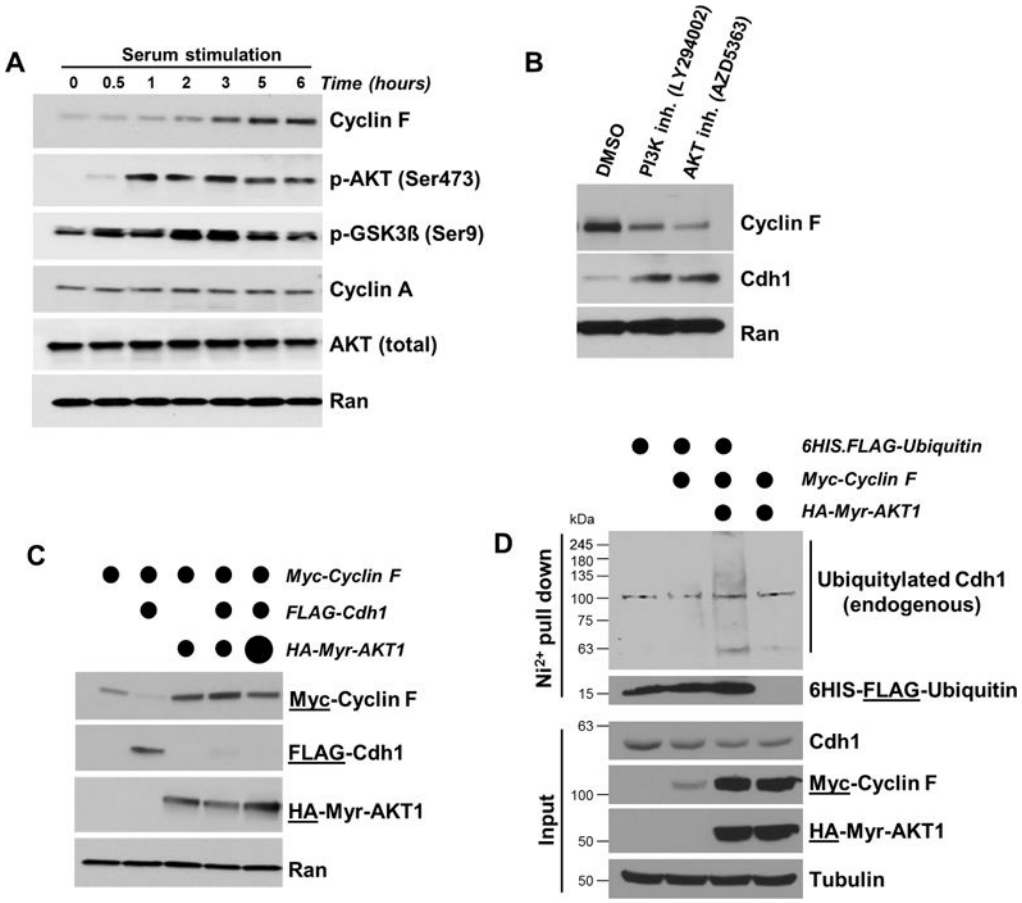

Figure 4. AKT promotes E3 ligase activity SCF(Cyclin F)

(A) Serum starvation and refeeding of HCT116 cells increases AKT activity and Cyclin F levels in a time-dependent manner.

(B) Pharmacological inhibition of PI3K or AKT kinases for six hours reduces Cyclin F protein levels in HeLa cells.

(C) The introduction of AKT1 stabilizes Cyclin F and promotes degradation of Cdh1. FLAG-Cdh1, Myr-HA-AKT1, and Myc-Cyclin F were co-expressed in various combinations.

(D) Myc-Cyclin F, FLAG-Cdh1, and 6HIS-ubiquitin were expressed in 293T cells, and ubiquitin conjugates were recovered on nickel agarose under denaturing conditions. Ubiquitylation of Cdh1 was analyzed by immunoblot. Cells were treated with MG-132 prior to harvesting and lysis.

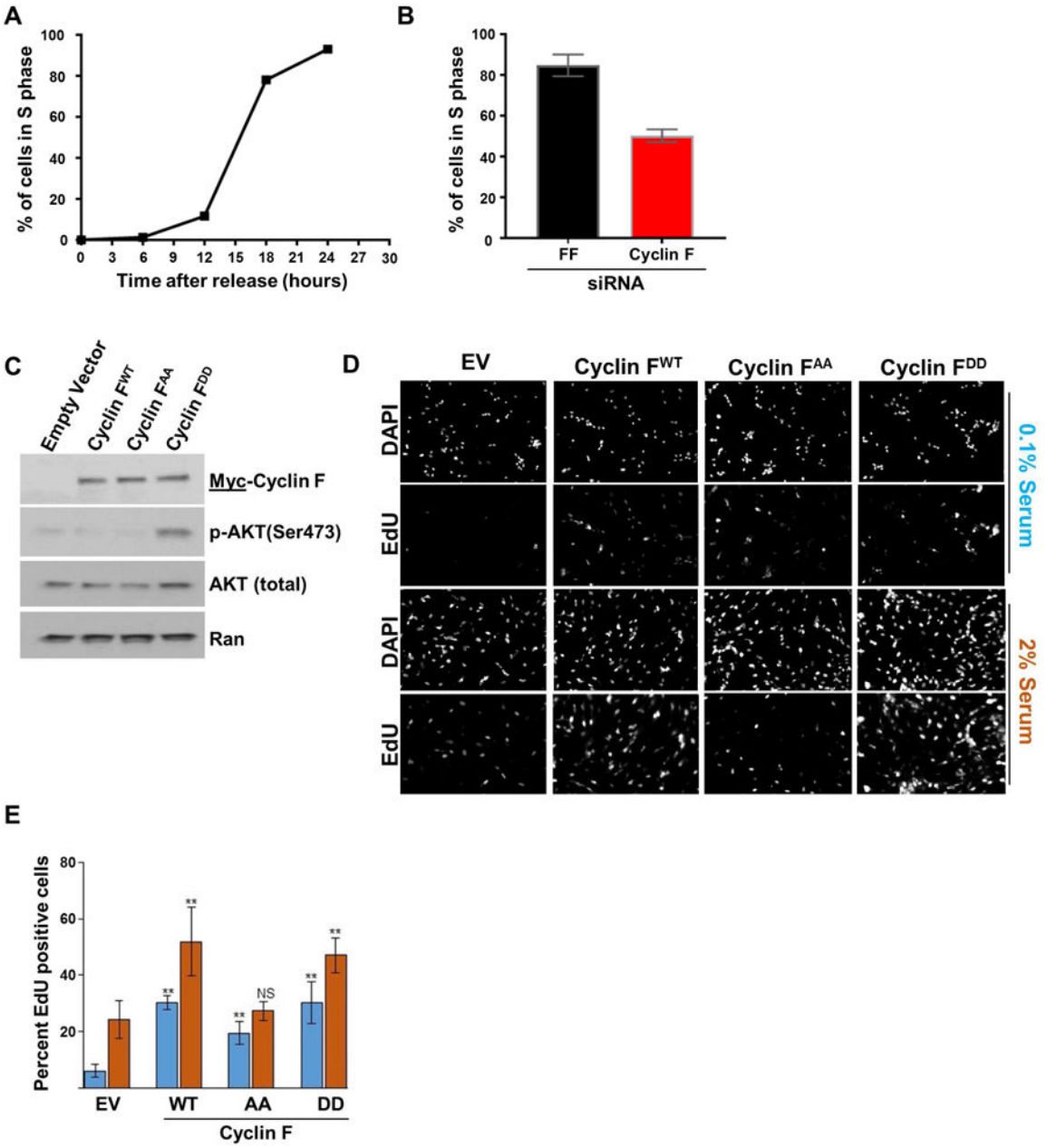

Figure 5. Cyclin F phosphorylation is required for G1/S progression

(A) Non-transformed RPE1 cells were synchronized in G0/G1 by serum withdrawal. After refeeding, entry in S-phase was monitored using EdU labeling.

(B) Depletion of Cyclin F with siRNA decreases S-phase entry.

(C) RPE1 cells were transfected with various versions of Cyclin F (WT, AA, DD) and then synchronized in G0/G1 as in panel A. Immunoblot of RPE1 cells overexpressing different Cyclin F mutants, prior to refeeding, is shown.

(D) After refeeding, cells were pulse labeled with EdU, fixed, and analyzed for S-phase entry. Representative images and DNA staining (top) of EdU positive cells (bottom) are shown.

(E) The percent of nuclei that are EdU positive is shown (performed in triplicate, * $p \leq 0.01$; ** $p \leq 0.004$; NS= not significant, p values were calculated using un-paired t-test). No serum control is shown in blue while the orange bar depicts 2% serum refeeding.